

Chapter 3

Isotope Effect in high temperature superconductors

3.1 Introduction

Historically the isotope effect has been in understanding the mechanism responsible for Cooper pair formation in conventional superconductors. It gives the response of T_c to an isotopic mass (M) change in the system and therefore gives information on how the dynamics of the ions are involved in the value of T_c . The experimental results [5] found that the average atomic mass M and the critical temperature T_c are fitted by a relation of the form $M^\alpha T_c = \text{constant}$, where α is the isotope effect coefficient. This relation can be written in the form $T_c = \text{constant} \cdot M^{-\alpha}$. In BCS theory with a pure phonon mechanism in the weak coupling limit, the expression for T_c can be written in the form $k_B T_c = 1.14 \hbar \omega_D \exp[-1/N(\mathbf{0})V]$. Since ω_D itself scales with the average atomic mass M like $M^{-1/2}$ so one find that $T_c = \text{constant} \cdot \omega_D = \text{constant} \cdot M^{-1/2}$ which cause the isotope exponent α to the theoretical value of $1/2$.

This simple picture, however, was somewhat spoiled by more elaborate experiments which showed that the isotope exponent, if indeed close to value of $1/2$, nevertheless deviated markedly from this ideal value in large number of materials. Some scope of agreement between theory and experiment could be restored by including the Coulomb interaction between the electrons in a more realistic that that used by BCS. Calculations by Morel and Anderson [14], which do not cut off the Coulomb repulsion arbitrarily at $\hbar \omega_D$ but rather at a much larger energy, lead to deviations from the ideal $1/2$ value that are in fairly good agreement with the observations. The key point is that any purely electronic (pairing) interaction between the electrons in a BCS condensate, whether repulsive or attractive, will cause the isotope exponent to deviate from its ideal $1/2$ value.

It is necessary to introduce the competition between electron-phonon interaction and the coulomb repulsions. This allows for negative values of α in agreement with experiment but only if T_c is of order 1 K or less[31]. Such a result is

inconsistent with the conventional electron-phonon model which was soon abandoned in favour of an electronic model. A joint phonon, but largely electronic mechanism is natural and explains the small values of α quite directly. Many such models are now on the market but none are as yet completely accepted.

In order to understand the origin of high- T_c and anomalous normal state properties of cuprate oxide superconductors several models have been proposed. Out of those the Van Hove singularity (VHS) scenario is one which is based on the phonon-mediated BCS pairing mechanism. Several groups [Refs.56-61] have investigated the role of the VHS in the density of states (DOS) on the transition temperature (T_c), the isotope exponent (α), and other properties within the BCS phonon-mediated pairing mechanism. Tsuei et al. [57] first tried to explain the anomalous isotope effect, observed in the La-214 system, on the basis of this model. Using approximate formulas for T_c and α , they obtained a minimum value of α when T_c is maximum. The DOS used in Refs.56-61 however, is an approximate one and not exactly derived from a Hamiltonian with realistic parameters.

In recent years it became apparent that the physics of underdoped high- T_c superconductors is governed by the pseudogap phenomenon. The underdoped high- T_c superconductors cuprates are characterized by the presence of hole correlations in the normal state giving rise to a pseudogap and a reduced density of states above T_c . It has been suggested that the isotope effect may reside wholly in the pseudogap and not in the superconductivity [62].

In the following we will study the influence of such a pseudogap on the isotope effect with the VHS in the electronic density of states by considering the s- and d-wave symmetries of the superconducting order parameter.

3.2 The Van Hove Scenario

It is well known that the quasi-two-dimensionality of the CuO planes in high-temperature superconductors gives rise to the logarithmic Van Hove singularities (VHS) in the electronic density of states (DOS). It has been shown that the incorporation of a VHS to the otherwise by standard BCS theory leads to quantitatively different results from those obtained using a constant DOS [56-59]. Moreover, this VHS model can

explain some important features in the high- T_c oxides, such as the high critical temperatures and the variation of the isotope exponent with doping. Tseui et al.[57] have given recent thermodynamics data to support the existence of a VHS near E_f in $\text{YBa}_2\text{Cu}_3\text{O}_7$. Within this scenario, Xing et al. [58] have given a good description of the cuprates with the weak-coupling BCS phonon-mediated pairing, of the variations in (a) the maximum in T_c , (b) the width of the T_c maximum, and (c) the isotope-shift minimum with doping. Getino et al.[59] derived an exact T_c formula within the VHS scenario of the BCS phonon-mediated pairing theory consisting of a logarithmic singularity in the density of states at the Fermi energy. Sarkar and Das [60] derived an exact expression for the isotope-shift exponent and the pressure coefficient of the transition temperature from the BCS gap equation for a DOS with the VHS. The isotope-shift exponent was also studied by Sarkar and Das [60] within the VHS scenario.

3.3 Van Hove Singularity in the Density of States

To investigate the nature of a saddle point in the energy surface which provides the divergence of the electron density of states, we begin with the expression of the density of states

$$N(E) = \frac{1}{(2\pi)^3} \int d^3\bar{k} \delta(E - E(\bar{k})). \quad (3.1)$$

Alternatively, the number of states in the energy interval between E and $E+dE$ is given by

$$N(E)dE = \int \frac{dS}{(2\pi)^3} \delta\bar{k}. \quad (3.2)$$

where S is the energy surface perpendicular to $\delta\bar{k}$. Since the infinitesimal change of $E(\bar{k})$ with respect to $\delta\bar{k}$ is given by

$$dE = \nabla_{\bar{k}} E \delta\bar{k}. \quad (3.3)$$

where $\nabla_{\bar{k}}$ means the gradient in \bar{k} -space. Thus we obtain the electron density of states as:

$$N(E) = \int \frac{dS}{(2\pi)^3} \frac{1}{|\nabla_{\bar{k}} E|}. \quad (3.4)$$

When $E(\bar{k})$ approaches zero, the density of states diverges. This is known as Van Hove singularities.

Let us consider an orthorhombic lattice as a simplified model of the high- T_c Cu-O oxides. Its band structure is assumed to be modeled by a tight-binding band [78]

$$E(\bar{k}) = -2t(\cos k_x + t_b \cos k_y) + 4t_2 \cos k_x \cos k_y - 2t' \cos k_z \quad (3.5)$$

Here t, t_b , and t' are the hopping integrals between nearest-neighbor Cu sites, respectively, along the a, b , and c axes, respectively, and t_2 is the hopping matrix element of the next-nearest-neighbor ones on the same Cu-O planes. D.Y.Xing et al.[79] introduce a set of dimensionless variables: $r_1=t_b/t$, $r_2=2t_2/t$, and $r' = t'/t$. For the system under consideration, the anisotropic parameter r' is assumed to be much smaller than unity ($r' \ll 1$), indicating that the interplanar hopping is very small compared with the intraplanar one. r_1 stands for the anisotropy within the Cu-O planes. Its introduction stems from the fact [80] that the high- T_c superconducting samples are often in the orthorhombic phase in which there is a slight difference in length between the lattice parameters along the a and b axes. So we can assume that r_1 is very close to, but slightly smaller than unity. Since t_2 is always much smaller than t , it is reasonable to assume that $r_2 < r_1$.

We first neglect the interplanar hopping (letting $t'=0$) and study the case of a 2D rectangular lattice. The corresponding electron density of states is given by the expression

$$N(E) = \pi^{-2} \int_0^\pi dk_x \int_0^\pi dk_y \delta(E - 2tW(k_x, k_y)), \quad (3.6)$$

where $W(k_x, k_y) = -\cos k_x - r_1 \cos k_y + r_2 \cos k_x \cos k_y$. We make a change of variables into v and w : $v = \cos k_y$ and $w = W(k_x, k_y)$. The δ function can be integrated over w , so the remaining integral over v is

$$N(E) = \frac{1}{2t\pi^2} \int_{v_1}^{v_2} \frac{dv}{\sqrt{1-v^2} \left| (1-r_2v^2) - (\varepsilon + r_1v)^2 \right|} \quad (3.7)$$

with $\varepsilon = E/(2t)$. Here the upper and lower integration limits of the integral are

$$v_2 = \min[1, (1 - \varepsilon)/(r_1 + r_2)] \quad (3.8)$$

$$v_1 = \max[-1, -(1 + \varepsilon)/(r_1 - r_2)]$$

It then follows that there may be three kinds of integration limits in Eq.(3.7). They are $v_1=-1, v_2=(1-\varepsilon)/(r_1+r_2)$ for $1+r_1+r_2 \geq \varepsilon \geq 1-r_1-r_2$; $v_1=-1, v_2=1$ for $1-r_1-r_2 \geq \varepsilon \geq -1+r_1-r_2$; and $v_2=1, v_1=-(1+\varepsilon)/(r_1-r_2)$ for $-1+r_1-r_2 \geq \varepsilon \geq -1-r_1+r_2$, respectively. Making use of the integral formula (3.147.5) of 81, we obtain the analytical expressions for $N(E)$ as

$$N(E) = \frac{1}{2t\pi^2 \sqrt{r_1+r_2\varepsilon}} K \left[\frac{\sqrt{(1+r_1)^2 - (\varepsilon-r_2)^2}}{\sqrt{4(r_1+r_2\varepsilon)}} \right] \quad (3.9)$$

for $1+r_1+r_2 \geq \varepsilon \geq 1-r_1-r_2$ or $-1+r_1-r_2 \geq \varepsilon \geq -1-r_1+r_2$, and

$$N(E) = \frac{1}{t\pi^2 \sqrt{(1+r_1)^2 - (\varepsilon-r_2)^2}} K \left[\frac{\sqrt{4(r_1+r_2\varepsilon)}}{\sqrt{(1+r_1)^2 - (\varepsilon-r_2)^2}} \right] \quad (3.10)$$

for $1-r_1-r_2 \geq \varepsilon \geq -1+r_1-r_2$, where $K(x) = F(\pi/2, x)$ is the complete elliptic integral of the first kind[36]. According to Eqs.(3.9) and (3.10), $N(E)$ is shown as a function of ε in Figure 1, in which the $N(E)$ exhibits two singular peaks at $\varepsilon_+ = 1-r_1-r_2$ and $\varepsilon_- = -1+r_1-r_2$. Taking into account the asymptotic formula $K(x) \approx \ln[4(1-x^2)^{-1/2}]$ with $x \approx 1$, we obtain for $N(E)$, near the singularities ε_{\pm} , the approximate expression

$$N(E) = \frac{1}{2t\pi^2 \sqrt{(1 \mp r_2)(r_1 \pm r_2)}} \ln \left[\frac{8\sqrt{(1 \mp r_2)(r_1 \pm r_2)}}{\sqrt{2(\varepsilon - \varepsilon_{\pm})(1-r_1)}} \right] \quad (3.11)$$

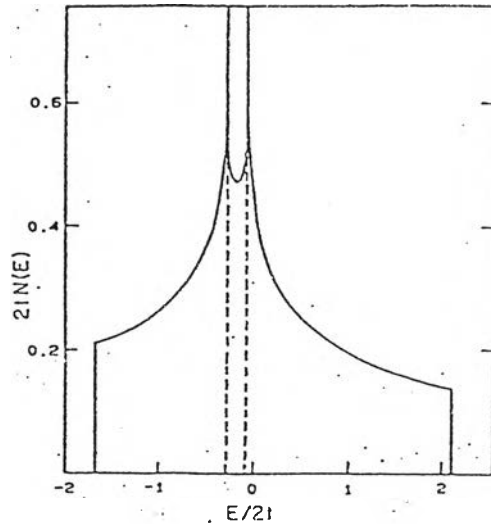


Figure 3-1a : Density of states, $N(E)$, for $r_1 = 0.9$ and $r_2 = 0.2$. The singularities occur for $\varepsilon_+ = 1-r_1-r_2 = -0.1$ and $\varepsilon_- = -1+r_1-r_2 = -0.3$. [58]

It can be seen from Figure 3-1a that the appearance of two singularities in $N(E)$ originated from the orthorhombicity of structure ($r_1 \neq 1$), the distance between them being equal to $\mathcal{E}_+ - \mathcal{E}_- = 2(1-r_1)$. As the rectangular to square lattice transition occurs (i.e., $r_1 = 1$), double Van Hove singularities at \mathcal{E}_+ and \mathcal{E}_- merge into a single one at $\mathcal{E}_+ = \mathcal{E}_- = -r_2$ [82], which is just the most used model[57,78]. We can conclude that the orthorhombicity of the structure leads to two sharp peaks in $N(E)$, but it does not change the logarithmic Van Hove singularity so long as the interplanar hopping is weak enough to be negligible.

We now turn our attention to the role of the Van Hove singularity given by Eqs. (3.9) and (3.10) in determining the magnitude of T_c and α . The density of states near this singularity has the following form:

$$N(E) = N_0 \left[\ln \left| \frac{E_F}{E - E_s} \right| + C \right], \quad (3.12)$$

$$\text{with } N_0^{-1} = 2t\pi^2 (1 - r_2^2)^{1/2}, \quad (3.13)$$

$$C = \ln \left| 16t (1 - r_2^2)^{1/2} / E_F \right|, \quad (3.14)$$

$$E_s = 2t\mathcal{E}_\pm. \quad (3.15)$$

To see the role of the $N(E)$ in determining the magnitude of T_c and α , we substitute Eq.(3.12) into the standard BCS gap equation, and obtain

$$\frac{2}{N_0 V} = \int_0^{k_B T_{co}} \frac{dy}{y} \tanh \left[\frac{y}{2k_B T_c} \right] \left[\ln \left| \frac{E_F^2}{y^2 - \delta^2} \right| + 2C \right] \quad (3.16)$$

where $y = E - E_F$, $\delta = E_F - E_s$, $k_B T_{co}$ is the maximum phonon frequency, and V is a measure of the electron-phonon interaction strength. Since the Fermi level is located right at Van Hove singularity ($\delta = 0$), from Eq.(3.16), an analytic expression for T_c can be obtained if the $\tanh(y/2k_B T_c)$ is approximated by the minimum between 1 and $(y/2k_B T_c)$:

$$T_c = 1.36 T_F \exp \left(C - \sqrt{2 / (N_0 V)} - 1 + [C + \ln(T_F / T_{co})]^2 \right) \quad (3.17)$$

where the Fermi temperature $T_F = |E_F| / k_B$.

The isotope-mass exponent α as defined in the expression $T_c \sim M^{-\alpha}$ can be calculated by

$$\alpha = -(\partial \ln T_c / \partial \ln M) = \frac{1}{2}(\partial \ln T_c / \partial \ln T_{co}). \quad (3.18)$$

where the relation $T_{co} \sim M^{-1/2}$ has been used. Based on the well-known BCS formula, $T_c \sim T_{co} \exp(-1/N_0 V)$, the BCS standard value for α is $1/2$. To determine the effect of the Van Hove singularity on α , we differentiate Eq.(3.16) with respect to T_{co} and perform the integral over y in the differential expression for $d \ln T_c / d \ln T_{co}$ by use of the approximations: $\tanh(y/2k_B T_c) \approx \min(1, y/2k_B T_c)$ and $\text{sech}(y/2k_B T_c) \approx \theta(2k_B T_c - y)$, where θ is the usual unit-step function. We finally obtain the analytical expression for α :

$$\alpha = 0.5 \frac{2C + \ln(E_F^2 / |k_B^2 T_{co}^2 - \delta^2|)}{2C + \ln[e^2 E_F^2 / (2k_B T_c)^2 - \delta^2] + (\delta / 2k_B T_c) \ln|(\delta - 2k_B T_c) / (\delta + 2k_B T_c)|} \quad (3.19)$$

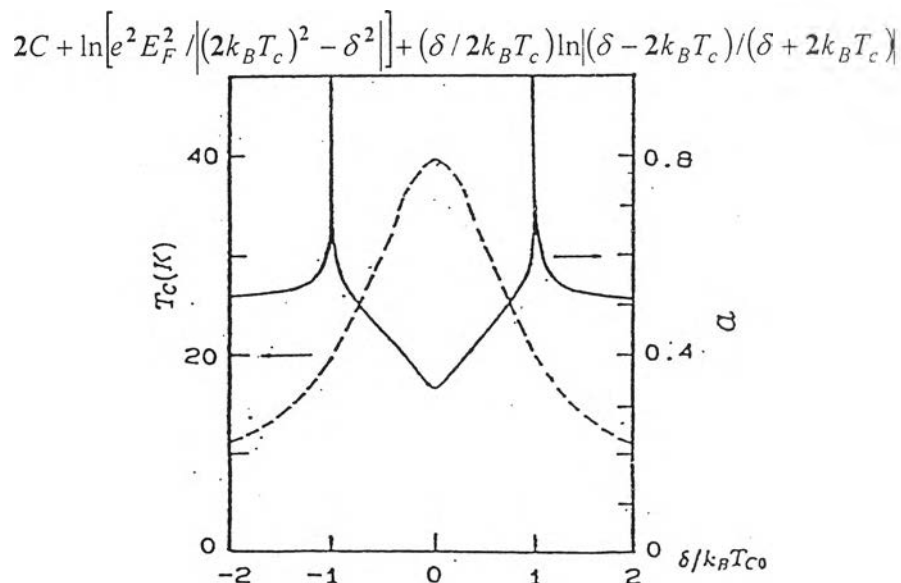


Figure 3-1b: Calculated results of T_c and α based on Eqs.(3.16) and (3.19) as a function of the Fermi-energy shift δ normalized to the phonon cut off energy $k_B T_{co}$ [79].

It appears to us that the symmetry in $\alpha(x)$ arises from the symmetry in $N(E)$ with respect to the single singularity, as given by Eq.(3.12). As the orthorhombicity of the structure is considered, the density-of-states function $N(E)$ has a couple of singularities. It has not been clear whether the asymmetry in $\alpha(x)$ is related to the orthorhombicity of the structure.

3.4 Isotope effect in high-temperature superconductors within Van Hove scenario

High- T_c Cu oxides such as $\text{YBa}_2\text{Cu}_3\text{O}_7$ and Bi-Sr-Ca-Cu-O systems are characterized by a near-zero oxygen-isotope effect. Recent results by Crawford et al. [87] show that the isotope effect in the $\text{La}_{2-x}\text{Sr}_x\text{CuO}_4$ system depends strongly on the doping level (x) and can significantly exceed the BCS limit. Within the framework of the BCS phonon-mediated pairing, Tsuei et al. [57] studied the role of a logarithmic (2D) van Hove singularity in the density of states provided a basis for understanding these anomalous isotope effects and possibly the origin of high-temperature superconductivity. They assumed a logarithmic density of states,

$$N(E) = N_0 \ln|E_F / (E - E_F)|. \quad (3.20)$$

where N_0 is the density of states normalized to a flat band with a bandwidth of $2E_F$. For the essence of the van Hove-singularity effects of T_c and the isotope effect, it will suffice to recall the standard BCS gap equation:

$$\frac{2}{V} = \int_{E_F - \hbar\omega_c}^{E_F + \hbar\omega_c} \tanh\left[\frac{E - E_F}{2k_B T_c}\right] N(E) \left(\frac{dE}{E - E_F}\right). \quad (3.21)$$

where ω_c is the cutoff frequency ($\hbar\omega_c \sim k_B T_{co}$), T_{co} is the phonon cutoff temperature, and V is a measure of the electron-phonon interaction strength.

From Eqs.(3.20) and (3.21), an expression for T_c can be obtained if the $\tanh[(E-E_F)/2k_B T_c]$ in Eq.(3.21) is approximated by two conditions: One is $\tanh[(E-E_F)/2k_B T_c] = (E-E_F)/2k_B T_c$ for $|E-E_F| \leq 2k_B T_c$, the other is $\tanh[(E-E_F)/2k_B T_c] = 1$ for $|E-E_F| > 2k_B T_c$ and we obtain :

$$T_c = 1.36 T_F \exp\left\{-\left[\frac{2}{N_0 V} + \left(\ln \frac{k_B T_F}{\hbar\omega_c}\right)^2 - 1\right]^{1/2}\right\}. \quad (3.22)$$

In the standard BCS treatment, $N(E)$ is assumed to be independent of energy, N_0 , and Eq.(3.21) will lead to the well-known BCS formula for T_c in the weak-coupling limit :

$$T_c = 1.13 T_{co} \exp(-1/N_0 V) \quad \text{for} \quad N_0 V \ll 1 \quad (3.23)$$

Estimate of T_c values based on Eqs.(3.22) and (3.23), using realistic parameters for the coupling constant, T_{co} , and T_F are listed in Table 3-1

	N_0V	T_{co} (K)	T_F (K)	T_c (K)
BCS with van Hove singularity	0.081	754	5800	40
	0.12	754	5800	92
Standard BCS	0.081	754	...	0.004
	0.12	754	...	0.2

Table 3-1: T_c estimates based on Eqs.(3.22) and (3.23) [57].

The effect of the Van Hove singularity on the isotope mass exponent α as defined in the expression $T_c \sim M^{-\alpha}$ can be calculated from Eq.(3.18). If the Fermi level is located right at the Van Hove singularity, α value will be [57]

$$\alpha_s = 0.5 \left[\ln \left(\frac{T_F}{T_{co}} \right) / \ln \left(\frac{1.36T_F}{T_c} \right) \right] \quad (3.24)$$

If the Fermi level is slightly off the singularity, then the T_c formula Eq.(3.22) becomes

$$T_c \approx 1.36T_F \exp \left(- \left[\frac{2}{N_0V} + \left(\ln \frac{T_F}{T_{co}} \right)^2 - 1 + \frac{\delta^2}{2k_B^2} \left(\frac{1}{4T_c^2} + \frac{1}{T_{co}^2} \right) \right]^{1/2} \right) \quad (3.25)$$

and consequently, Eq.(3.24) is modified as

$$\alpha \approx 0.5 \left[\left(\ln \left(\frac{T_F}{T_{co}} \right) + \frac{\delta^2}{2k_B^2 T_{co}^2} \right) / \left(\ln \left(\frac{1.36T_F}{T_c} \right) - \frac{\delta^2}{8k_B^2 T_c^2} \right) \right] \quad (3.26)$$

where δ is the E_F shift from the singularity and it is assumed that $\delta < 2k_B T_c$.

From Eqs.(3.22), (3.24), (3.25) and (3.26), one concludes that a logarithmic Van Hove singularity in $N(E)$ at or very close to the Fermi level can indeed significantly decrease α from its standard BCS value = 0.5. In particular, Eqs.(3.25) and (3.26) show that α is at minimum when T_c is maximum [57]. This is qualitatively in agreement with

the α data shown in Figure3-2. It should be pointed out that a Van Hove singularity in $N(E)$ can lead to the absence of the isotope effect in a weak-coupled BCS superconductor.

Sarkar and Das [60] investigated the isotope exponent within the Van Hove scenario, using the BCS equation for the gap energy at finite temperature for a general density of states $N(\mathcal{E})$. The standard equation is

$$\frac{2}{V} = \int_{\mathcal{E}_F - \omega_D}^{\mathcal{E}_F + \omega_D} N(\mathcal{E}) \frac{1}{\sqrt{(\mathcal{E} - \mathcal{E}_F)^2 + \Delta^2(T)}} \tanh \frac{\sqrt{(\mathcal{E} - \mathcal{E}_F)^2 + \Delta^2(T)}}{2T_c} d\mathcal{E} \quad (3.27)$$

They assumed a density of states (DOS) with a van Hove singularity as

$$N(\mathcal{E}) = N_0 \ln \left| \frac{\mathcal{E}_F - \delta}{\mathcal{E} - (\mathcal{E}_F - \delta)} \right| \quad (3.28)$$

where δ is the Fermi level shift.

The DOS (3.28) has some relevance in the context of high- T_c cuprate oxides. The success of van Hove scenario lies in the assumption that δ is zero for the optimum doping concentration for which T_c is maximum.

The equation for the transition temperatures for the DOS(3.28) is obtained from Eqs. (3.27) and (3.28) using the condition $\Delta(T) = 0$ at $T = T_c$,

$$\frac{2}{N_0 V} = \int_{-\omega_D}^{\omega_D} \frac{1}{x} \tanh \left(\frac{x}{2T_c} \right) \ln \left| \frac{\mathcal{E}_F - \delta}{x + \delta} \right| dx, \quad (3.29)$$

where $x = \mathcal{E} - \mathcal{E}_F$.

Approximating $\tanh(x/2T_c) = x/2T_c$ for $x/2T_c \leq 1$ and $\tanh(x/2T_c) = 1$ for $x/2T_c > 1$ in Eq.(3.29) Tseui et al. [12] obtained an approximate formula for T_c , expressed in Eq. (3.22).

Getino et al. [59] proceeded further by integrating the right hand side of Eq. (3.29) by parts to obtain an intrinsic equation for T_c which has to be solved for T_c numerically and self-consistently.

Sarkar and Das [60] determined T_c directly from Eq. (3.29) by numerically integrating the right-hand side of the equation and obtain T_c values which are the same as those determined by Getino et al. [59] and almost 16 % lower than those obtained

from formula (3.22) for the same set of parameters. In Table 3-2 they have compared the T_c values as determined by them and from Eq. (3.25)-(3.26). The T_c versus δ plot is shown in Fig.3-2 [60], we can see that T_c is maximum at $\delta = 0$ and decreases as $|\delta|$ increases, i.e., as the Fermi level shifts from the energy of the VHS. T_c decreases for $\delta < 0$ slightly more rapidly than for $\delta > 0$. It may be mentioned that T_c falls symmetrically about $\delta = 0$ within the approximate formula (3.22).

N_0v	ϵ_F (K)	ω_D (K)	T_c (K) (Ref.12)	T_c (K) (Present study)	α (Present study)
0.084	5800	754	43.8	37.7	0.197
0.10	5800	754	64.1	55.2	0.213
0.12	5800	754	91.8	79.4	0.231

Table3-2: T_c estimates for a DOS with a VHS at the Fermi level ($\delta = 0$), (a) using the approximate T_c formula of 12, and (b) Sarkar and Das 's investigation. Values of the isotope-shift exponent (α) are also given.[60]

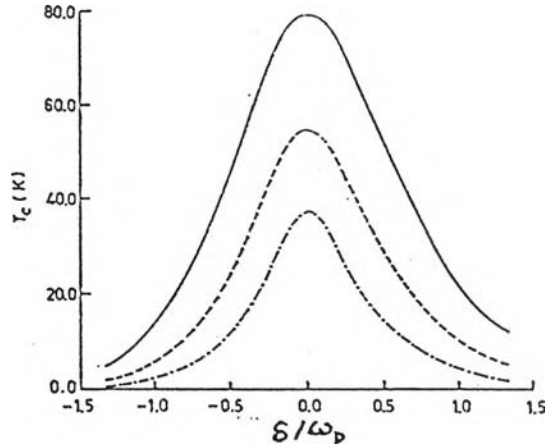


Figure 3-2: Variation of the transition temperature (T_c) with δ/ω_D for different coupling parameters: solid line ($N_0v=0.12$), dashed line ($N_0v=0.10$), and dot-dashed line ($N_0v=0.084$), $\epsilon_F=5800$ K, $\omega_D=754$ K [15].

The isotope-shift exponent α is defined as

$$\alpha = - \left(\frac{\partial \ln T_c}{\partial \ln \omega_D} \right) \left(\frac{\partial \ln \omega_D}{\partial \ln M} \right) = 0.5 \left(\frac{\partial \ln T_c}{\partial \ln \omega_D} \right), \quad (3.30)$$

where the relation $\omega_D \propto M^{-0.5}$ is used. The standard BCS theory predicts $\left(\frac{\partial \ln T_c}{\partial \ln \omega_D} \right) = 1$

and correspondingly $\alpha = 0.5$. To determine the isotope-shift exponent (α) for the density of states (3.28) one has to differentiate Eq.(3.29) with respect to ω_D . An exact expression for α is hence obtained [60],

$$\begin{aligned}\alpha &= 0.5 \frac{\partial \ln T_c}{\partial \ln \omega_D} \\ &= \frac{1}{I} \left[T_c \tanh\left(\frac{\omega_D}{T_c}\right) \ln \left| \frac{(\epsilon_F + \delta)^2}{\omega_D^2 - \delta^2} \right| \right],\end{aligned}\quad (3.31)$$

where

$$I = \int_{-\omega_D}^{+\omega_D} \text{sech}^2(x/2T_c) \ln \left| \frac{\epsilon_F + \delta}{x - \delta} \right| dx \quad (3.32)$$

The values of α are determined for various δ values and for different sets of parameters by numerically evaluating the integration in Eq. (3.18). The α versus δ plots are shown in Figure 3-3 for different coupling strengths. α is minimum when $\delta=0$, i.e., when the Fermi level is at the VHS and T_c is maximum. As the Fermi level shifts from the VHS, α increases with $|\delta|$ where it shows a maximum and then decreases (Fig. 3-3). The shape of the α versus δ curve is very similar to that obtained by Tsuei et al.[12], but Sarkar and Das [15] obtained higher values of α . For $N_0V = 0.084$ Tsuei et al. Obtained $\alpha \sim 0.15$ whereas Sarkar and Das obtained $\alpha = 0.192$. Figures 3-2 and 3-3 show that, although T_c is widely different for the three sets of parameters, the values of α are almost the same for the different sets except near $\delta=0$. In the neighborhood of $\delta=0$, we obtain a lower value of α for lower value of N_0V .

From Figures 3-2 and 3-3 it is seen that α is minimum at optimum doping when $T_c=T_c^{\max}$ and α is higher for low T_c samples (underdoped or overdoped). The behavior of α within the VHS scenario thus agrees qualitatively with the experimental results of high- T_c oxides, as pointed out by Tsuei et al. [12]. However, the experimental values of α for cuprate systems with higher T_c (e.g., Y-1:2:3, Bi-2:2:1:2) at optimum doping are much less than those obtained in Tsuei et al.'s study.

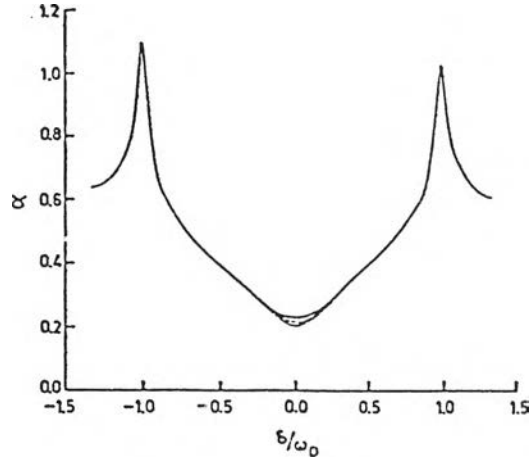


Figure 3-3: Plot of the isotope exponent α vs (δ/ω_D) . solid line ($N_0V = 0.12$), dashed line ($N_0V = 0.10$), and dot-dashed line ($N_0V = 0.084$), $\mathcal{E}_F = 5800$ K, $\omega_D = 754$ K [60].

A. Gama Goicochea [86] investigated how the isotope exponent was effected by the influence of a logarithmic Van Hove singularity in the electronic density of states within the framework of the BCS theory, he used the following 2D-VHS form for the DOS

$$N(\mathcal{E}) = N_0 \left[\ln \left| \frac{\mathcal{E}_F}{\mathcal{E} + \delta} \right| + C \right] \quad (3.33)$$

where \mathcal{E} is the energy, referred to \mathcal{E}_F , N_0 is the density of state at the Fermi level as a normalization factor and δ is the so-called filling factor which sets the position of the singularity with respect to the Fermi energy. From the linearized BCS equation

$$\frac{2}{V} = \int_{-\omega_D}^{\omega_D} N(\mathcal{E}) \tanh\left(\frac{\mathcal{E}}{2k_B T_c}\right) \frac{d\mathcal{E}}{\mathcal{E}} \quad (3.34)$$

for a cutoff frequency ω_D , a constant pairing potential V , and introducing Eq.(3.33) for $N(\mathcal{E})$, one finds

$$k_B T_c = 1.36 \mathcal{E}_F \exp \left(C - \sqrt{\frac{2}{N_0 V} + \left[\ln \left(\frac{\mathcal{E}_F}{\omega_D} \right) + C \right]^2} + \frac{\delta^2}{2} \left[\frac{1}{(2k_B T_c)^2} + \frac{1}{\omega_D^2} \right] - 1 \right) \quad (3.35)$$

which provided significantly larger values for T_c than the standard BCS formula. Eq. (3.35) shows that T_c is maximum when $\delta = 0$, i.e. when the VHS is placed at the Fermi energy. An estimate of T_c using Eq(3.35) and the classical BCS formula,

$$k_B T_c = 1.13 \omega_D \exp[-1/N(\varepsilon_F)V], \text{ shows that } T_c^{VHS} \text{ is at least three orders of magnitude larger than } T_c^{BCS}.$$

Consider the isotope effect exponent α defined as

$$\alpha = -\frac{\partial \ln T_c}{\partial \ln M} = -\frac{\omega_D}{2T_c} \frac{\partial T_c}{\omega_D}, \quad (3.36)$$

where M is the isotopic mass, and the relation $\omega_D \sim M^{-1/2}$ has been used. Thus, differentiating Eq.(3.34) with respect to ω_D and then the integration over energies yields

$$\alpha = 0.5 \left[\frac{\ln(\varepsilon_F^2 / |\omega_D^2 - \delta^2|) + 2C}{\ln(\varepsilon_F^2 / |(2k_B T_c)^2 - \delta^2|) + (\delta / 2k_B T_c) \ln \left| \frac{\delta - 2k_B T_c}{\delta + 2k_B T_c} \right| + 2C + 2} \right] \quad (3.37)$$

A numerical calculation of α based on Eqs. (3.34) and (3.36) is shown in Figure 3-4 as a function of δ/ω_D , for different values of the constant background in the DOS, N_0C . As shown by both Eq.(3.37) and Figure 3-4, α has a minimum when T_c is maximum, i.e. , at $\delta = 0$. The peak in this figure corresponds to a singularity occurring when $|\delta| = \omega_D$, as can be easily seen in Eq.(3.37). Note that the lowest values for α are achieved only when the background N_0C is neglected, whereas for large δ it is found that α goes to the BCS limit, $\alpha = 0.5$. These conclusions are in agreement with Xing et al.[58] . Originally, Tsuei et al.[57] invoked a VHS to explain the isotope effect measurements by Crawford et al. [87] on the $\text{La}_{2-x}\text{Sr}_x\text{CuO}_{4-y}$ system as a function of doping x . However, early measurements [88] of the copper and oxygen isotope effect exponent in this system confirm that the minimum values of α (~0.0-0.17) are too small to be accounted for by a simple VHS approach. Experiments in other high- T_c materials seem to support this view [89-90]. The introduction of the

constant background N_0C appears to have a strong influence, for it raises the minimum values of α . Figure 3-5 shows α as a function of T_c for a VHS with and without the constant background, and the results are compared to recent experiments on the yttrium-based compounds. [86]

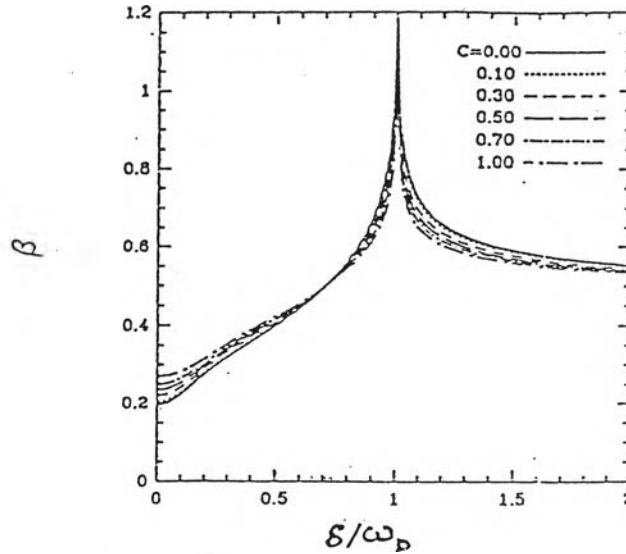


Figure 3-4: Isotope effect exponent as a function of δ/ω_0 for increasing values of constant C [Eq.(3.33)] , for $\mathcal{E}_F=500$ meV, $\omega_0 = 65$ meV, and $N_0V = 0.08$. [86]

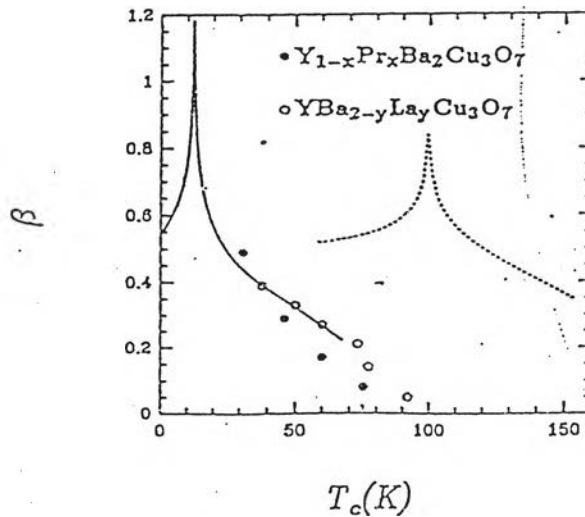


Figure 3-5: Isotope effect exponent as a function of T_c . The solid line corresponds to $C=0$, while the dotted line is for $C=2$. The parameters are kept the same as in Figure 3-4. Experimental data are taken from Franck et al. [89] (open circles) and Bornemann and Morris [90] (solid hexagons).

A.M. Shamuszaman and A.K.M.A. Islam [40] studied the isotope exponent (α) of some high T_c superconductors by using an exact expression for α for an

electronic density of state (EDOS) in the Van Hove Singularity Scenario (VHS). The results reproduce the general experiment trend of α as a function of doping (x) as follows

$$\alpha = \frac{1}{I} \left[T_c \tanh\left(\frac{\omega_D}{2T_c}\right) \ln \left| \frac{E_F - \delta}{\omega_D^2 - \delta^2} \right| \right] \quad (3.38)$$

where

$$I = \int_{-\omega_b}^{\omega_b} \text{sech}^2\left(\frac{X}{2T_c}\right) \ln \left| \frac{E_F - \delta}{X + \delta} \right| dX \quad (3.39)$$

Eq.(3.38) is used to evaluate the isotope exponent (α) and the calculated value of α for $\text{YBa}_2\text{Cu}_3\text{O}_{6+x}$ as a function of doping (x) is shown in Figure 3-6. This result produces the general experimental trend of α as a function of doping (x).

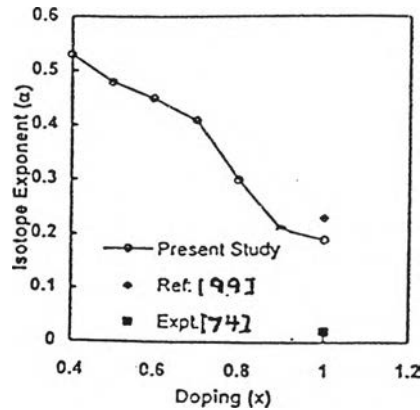


Figure 3-6: $\alpha \sim x$ curve for $\text{YBa}_2\text{Cu}_3\text{O}_{6+x}$ [85].

In Figure 3-6 the curve agrees with the experimental trend although optimum value ($\alpha=0.19$) is much larger than the experimental value ($\alpha=0.02$) [74]. Doping dependence of Debye temperature, transition temperature and the variation of Fermi level shift (δ) from the Van Hove singularity with doping(x) have been made in this work. δ is determined from T_c equation assuming that $\delta < 2k_B T_c$ therefore the overdoped region is not taken under consideration since $\delta < 2k_B T_c$ in this region.. The important features of the calculation are that δ has a minimum at the highest T_c and increases monotonically around T_c .

A. Bhardwaj and S. K. Muthu [91] studied the influence of singularities in the electronic density of states (DOS) on high temperature superconductors in the framework of the conventional BCS theory, by using a DOS with singularities at two different points. They could explain the asymmetry in the isotope exponent (α) with respect to the point where T_c is maximum. They considered a DOS with a Van Hove singularity of the form

$$N(E) = N_0 \ln \left| \frac{E_F}{E - E_F - \delta} \right| \quad (3.40)$$

where $\delta = -\delta_1$ for $E_F - \hbar\omega_D \leq E \leq E_F$
 $= \delta_2$ for $E_F \leq E \leq E_F + \hbar\omega_D$.

and $0 \leq \delta_1, \delta_2 \leq 2k_B T_c$.

The BCS gap equation is given by Eq.(3.21)

$$\frac{2}{V} = \int_{E_F - \hbar\omega_c}^{E_F + \hbar\omega_c} \tanh \left[\frac{E - E_F}{2k_B T_c} \right] N(E) \left(\frac{dE}{E - E_F} \right) \quad (3.41)$$

Using Eq.(3.40) one obtains ($\lambda = N_0 V$)

$$\frac{2}{\lambda} = I_1 + I_2 \quad (3.42)$$

$$\text{with } I_1 = \int_0^{\hbar\omega_D} \tanh \left(\frac{x}{2k_B T_c} \right) \ln \left| \frac{E_F}{x - \delta_1} \right| \frac{dx}{x} \quad (3.43)$$

$$\text{and } I_2 = \int_0^{\hbar\omega_D} \tanh \left(\frac{x}{2k_B T_c} \right) \ln \left| \frac{E_F}{x - \delta_2} \right| \frac{dx}{x} \quad (3.44)$$

To simplify the evaluation of I_1 and I_2 , we make the assumption $\tanh(u) \cong u$ for $u \leq 1$ and $\tanh(u) \cong 1$ for $u > 1$. A straightforward calculation yields the values of I_1 and I_2 when, coupled with Eq.(3.42) lead to the equation

$$2k T_c = eE_F \exp \left[- \left(\frac{2}{\lambda} - \left(\frac{\delta_1 + \delta_2}{2k_B T_c} \right) \ln(2e^2 k_B T_c) + \frac{1}{2k_B T_c} (\delta_1 \ln \delta_1 + \delta_2 \ln \delta_2) \right. \right. \\ \left. \left. + \left(\frac{\delta_1 + \delta_2}{\hbar \omega_D} \right) + \left(\frac{\delta_1^2 + \delta_2^2}{4} \right) \left(\frac{1}{4k_B^2 T_c^2} + \frac{1}{\hbar^2 \omega_D^2} \right) + \left(\ln \frac{E_F}{\hbar \omega_D} \right)^2 - 1 \right)^{1/2} \right] \quad (3.45)$$

where $e \approx 2.7183$

Next one calculates the isotope exponent α defined by $\alpha = -d \ln T_c / d \ln M$ and assuming that θ_D to be proportional to $M^{-1/2}$, one obtains from Eq.(3.45)

$$\alpha = \frac{0.5 \left[\ln \left(\frac{T_F}{\theta_D} \right) + \frac{x_1^2 + x_2^2}{4} + \frac{x_1 + x_2}{2} \right]}{\left[\ln \left(1.36 \frac{T_F}{T_c} \right) - \left(\frac{\theta_D}{4T_c} \right) x_1 \ln \left(\frac{\theta_D x_1}{2eT_c} \right) - \left(\frac{\theta_D}{4T_c} \right) x_2 \ln \left(\frac{\theta_D x_2}{2eT_c} \right) - \frac{\theta_D^2}{16T_c^2} (x_1^2 + x_2^2) \right]} \quad (3.46)$$

with $x_1 = \delta_1 / (k_B \theta_D)$ and $x_2 = \delta_2 / (k_B \theta_D)$.

For the particular case with $\lambda = 0.081$, $T_F = 5800$ K, and $\theta_D = 754$ K, these values have been used by Tsuei et al. [57] in their calculations and represent realistic values, one uses Eqs(3.45) and (3.46) to construct Table3-3 that gives the numerical values of T_c and α for two different choices of x_1 and x_2 .

(a) $x_1 = -x_2 = x$			(b) $x_2 = -4x_1 = x$		
x	T_c	α	x	T_c	α
-0.108	39.14	0.204	-0.105	35.12	0.206
-0.08	39.64	0.199	-0.08	35.96	0.203
-0.06	39.99	0.196	-0.06	36.68	0.202
-0.04	40.19	0.194	-0.04	37.51	0.200
-0.02	40.26	0.193	-0.02	38.55	0.198
0	40.19	0.194	0	40.26	0.193
0.02	39.99	0.196	0.06	43.20	0.191
0.04	39.64	0.199	0.12	43.40	0.202
0.06	39.14	0.204	0.18	42.00	0.227
0.08			0.24	38.59	0.293

Table 3-3: Values of T_c and α calculated from Eqs.(3.45) and (3.46) [91].

3.5 Effect of doping and impurities on the isotope effect in high-temperature superconductors

Early measurements on optimally doped samples [61-62] found an oxygen isotope effect coefficient almost zero, which was used as evidence that the pairing mechanism in the high-temperature superconductors (HTSC) is not phonon mediated. Later measurements revealed an oxygen isotope-effect coefficient that increased rapidly in going from the optimally doped (hole concentration $p=0.16$) to the underdoped region ($p<0.16$), reaching values greater than 0.5 [63-64]. This could not be accounted for by the simple inclusion of the Coulomb interaction, because small α values imply small T_c values which is the exact opposite of what is observed in the HTSC. D.J Pringle et al. [65] showed that the hole-concentration and impurity-concentration-induced changes in the isotope-effect coefficient can be consistently modeled by including the effect of the normal-state pseudogap. They have performed oxygen isotope-effect measurements on $Y_{1-x}Ca_xBa_2Cu_3O_7$ ($T_{c,max} \sim 90K$), $Bi_2Sr_2CaCu_2O_{8+\delta}$ ($T_{c,max} = 90K$), and $YBa_2(Cu_{1-x}Ni_x)_4O_8$ ($T_{c,max} = 81K$) and distinguish between the isotope effect in T_c , α_{Tc} , and that in the superconducting spectral gap α_{Δ} and also showed that the normal-state pseudogap can account for the rapid increase in the isotope effect coefficient with increasing Ni substitution in $YBa_2(Cu_{1-x}Ni_x)_4O_8$.

3.6 Physics of the pseudogap

To probe the properties of cuprates, condensed-matter physicists turned to a technique called angled-resolved photo-emission spectroscopy (ARPES). Below T_c , ARPES experiments reveal that the superconducting gap depends on the direction in which the photon is fired into the material. There is a large gap in some directions and a small gap in others [100-102]. This just reflects the d-wave nature of the pairs and fits in well with Landau's theoretical picture but when one heats the materials up above T_c , the energy gap does not go away. This anomaly is the pseudogap, and it makes a shambles of the conventional BCS theory. The pseudogap may provide one key, in 1995, Vic Emery and Steve Kivelson [67] pointed out that superconductivity requires phase coherence between those pairs, which each pair has a quantum wave associated with it, and for the pairs to condense into the superconducting state all the waves have

to be in phase with one another. As the pseudogap exists almost up to room temperature, it could be that some feature of cuprate structure makes it possible for pairs to form at high temperature, well above T_c . The onset of superconductivity would signify not the formation of pairs, but the setting in of phase coherence below T_c . In this view, cuprate superconductivity may break down above T_c because the pairs have much thermal energy that they can no longer maintain phase coherence. Emery and Kivelson suggest that, just above T_c , superconductivity should therefore become fragmented or fluctuating, it should be possible to find evidence of superconductivity in the material, but only very short distances or timescales.

In 1999, this idea won support from experiments by a team led by Joe Orenstein [103] studied how another type of cuprate $\text{Bi}_2\text{Sr}_2\text{CaCu}_2\text{O}_{8+x}$ responded to an electrical field that was alternating very rapidly. They found exactly the sort of fluctuations that Emery and Kivelson had predicted. Above T_c , the higher levels of thermal energy appeared to churn up small vortices regions in which the material became non-superconducting. In August, 2000 S. Uchida and his colleagues [104] found further evidence for such vortices. They showed that magnetic fields generally will not pass through a superconductor, but they can penetrate through non-superconducting vortices.

3.7 Isotope effect in the presence of a pseudogap

Many different models have been advanced in order to try to understand this unusual doping dependence in connection with the small isotope exponent at optimal doping. In recent years it became apparent that the physics of underdoped high- T_c superconductors is governed by the pseudogap phenomenon. A behavior which is reminiscent of the presence of a pseudogap, growing upon successive underdoping, has been observed consistently in a large number of different experiments, e.g., nuclear magnetic resonance (NMR) Knight-shift and relaxation rate experiments, specific heat, angled-resolved photoemission spectroscopy conductivity [61-62].

To clarify the origin of this pseudogap behavior, many proposals have been presented. These are roughly classified into the following groups. One of the suggestions that the pseudogap is caused by the singlet formation of spinons which

appears as a result of the spin-charge separation [64]. The others suggest that the pseudogap is related to instabilities in some ordering states. One of these is the theory [20-21] relating the pseudogap with the antiferromagnetic phase which is reached by controlling the doping or the pressure. The other is the theory [65-69] relating it with the superconducting phase which is reached by controlling the temperature. The first one assumes that the system cannot be described by the Fermi liquid theory. However, there is no positive reason to consider the two dimensional interacting electrons system as a non-Fermi liquid [70].

In the real system [63], it is observed that as temperature decreases, the pseudogap grows and then the pseudogap phase is connected with the superconducting phase but not with the antiferromagnetic phase. It is also observed in ARPES (angle-resolved photoemission spectroscopy) experiments that the symmetry of the pseudogap in the momentum space is the same as the symmetry of a Cooper pair [70]. Therefore it is important to investigate the phenomenon related with the pseudogap by taking the superconducting fluctuation into account.

On the basis of the superconducting fluctuation, the pseudogap state is investigated theoretically in two different ways. This difference partially originates from the interpretation of the superconducting phase transition. One of these theories [22-23] considers that the superconducting transition in these compounds is a Kosterlitz-Thouless transition because of the two dimensionality of the system. In this case the superconducting phase has a finite superfluid density but not necessarily the order parameter. It is known that the real systems has a finite transfer integral between layers. Therefore it is reasonable to consider that the superconducting transition is characterized by the Thouless criterion while the transition temperature (T_c) is much reduced from that of the mean field theory due to the strong two dimensionality. Actually the superconducting phase has an order parameter although its temperature dependence is not trivial due to the reduced T_c .

G.V.M. Williams et al.[71] have studied the absence of an isotope effect in the pseudogap in $\text{YBa}_2\text{Cu}_4\text{O}_8$ as determined by the high-resolution ^{89}Y NMR (nuclear magnetic resonance) and showed that an isotope effect occurs in T_c but not in the normal-state pseudogap. By taking account of the pseudogap, they also showed that

isotope effect coefficient in the superconducting gap parameter (α_{Δ}) remain small (≈ 0.06) and roughly constant, independent of hole concentration in spite of the large value of α_{T_c} in the underdoped region.

The key issues emerge from the presence of the pseudogap is the energy scale for superconductivity is set by Δ_0 , not by T_c , so the fundamental isotope exponent is not α_{T_c} but $\alpha_{\Delta} \equiv -d \ln \Delta_0 / d \ln M$. Indeed, it has been suggested that the isotope effect may reside wholly in the pseudogap and not in superconductivity [72]. Figure 3-7 summarizes these two cases within the model of Loram et al.[73] : (a) $\alpha_{\Delta} \neq 0$ while the isotope effect coefficient in the pseudogap energy scale E_g (α_{E_g}) = 0, and (b) $\alpha_{\Delta} = 0$ while $\alpha_{E_g} \neq 0$.

The isotope shift in T_c was measured by the zero-field cooled magnetization measurements using a vibrating sample magnetometer and an applied field of 5×10^{-4} T. The resultant magnetization curves are plotted in the inset of Figure 3-8 for ^{16}O (solid curve) and 90 % ^{18}O (dashed curve) Y124 samples, leading to $\alpha_{T_c} = (0.076 \pm 0.010)$, comparable to previous studies [74].

The presence of the pseudogap provides a simple explanation for the dependence of α_{T_c} on hole concentration p , as illustrated in Figure 3-7(a). In particular, the depression of T_c in spite of the nearly constant value of Δ_0 on the underdoped side, results in a divergence of α_{T_c} typical of what is observed [29], as shown in Figure 3-9 for $\text{Y}_{1-x}\text{Pr}_x\text{Ba}_2\text{Cu}_3\text{O}_7$, $\text{YBa}_{2-x}\text{La}_x\text{Cu}_3\text{O}_7$, and $\text{YBa}_2(\text{Cu}_{1-x}\text{Co}_x)_3\text{O}_7$ [29] This can be quantified using the model of Loram et al.[30] in which the spectral gap $\Delta(T)$ is related to the superconducting order parameter $\Delta'(T)$ by $\Delta^2(T) = \Delta'^2(T) + E_g^2(T)$ and T_c is the temperature at which $\Delta(T_c) = E_g(T_c)$. Thus, the experimentally observed increase in E_g with increasing underdoping [73,76] causes a reduction in Δ' and, hence, in T_c and a resultant increase in α_{T_c} . The data is modeled by noting that E_g can be written as $E_g/\Delta_0 = f(T_c/T_{c,0})$ and, hence, $T_c = T_{c,0}F(E_g/\Delta_0)$, where $F(x) = f^{-1}(x)$. Thus, taking $\Delta_0 = b_0 M^{\alpha_{\Delta}}$ and $T_{c,0} = \beta \Delta_0/k_B$, then

$$\alpha_{T_c}(Z) = \alpha_{\Delta} \left[\mathbf{1} - \frac{d \ln[F(y)]}{d \ln(y)} \right], \quad (3.47)$$

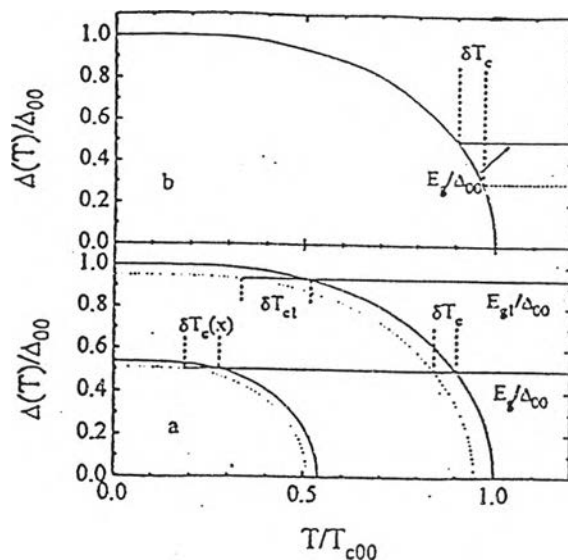


Figure 3-7 : Schematic plots of the temperature dependence of the d-wave gap maximum $\Delta(T)$ for ^{16}O isotope exchange (solid curves) and ^{18}O exchange (dotted curves). The horizontal lines are the temperature-independent pseudogap energy E_g . (a) isotope effect only in Δ_0 and not in E_g . The lower pair of curves show the effect of a reduced Δ_0 due to impurity pair breaking. (b) Isotope effect only in E_g and not in Δ_0 [71].

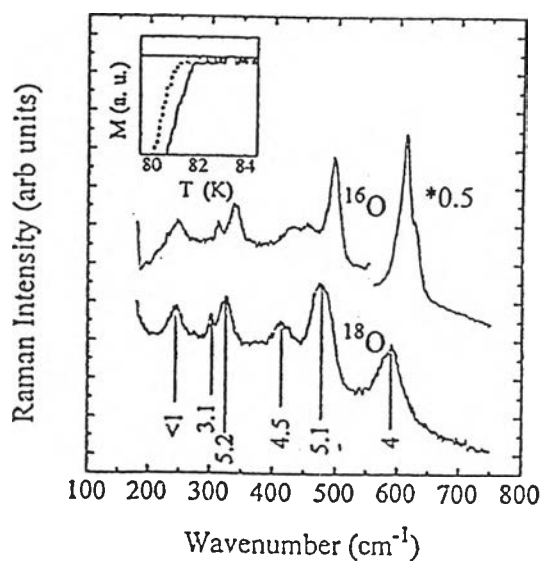


Figure 3-8 : Raman spectra from ^{16}O -exchanged and 90% ^{18}O -exchanged Y-124. The isotope-induced shifts in the phonon mode frequencies are shown in % for each mode. Inset: Magnetization plotted against temperature for the ^{16}O -exchanged (solid curve) and 90% ^{18}O -exchanged (dashed curve) Y124 samples [71].

where $z=2k_B T_c/E_g$, $y = E_g/\Delta_0 = f(T_c/T_{c,0})$. One can use the d-wave form of the BCS gap equation to obtain $f(T_c/T_{c,0})$ and, hence, $F(E_g/\Delta_0)$ and show in Figure 3-9 that this model can reasonably describe the data with $\alpha_\Delta = 0.06$, noting that for T_c near $T_{c,0}$, the asymptotic form of Eq.(3.47) is $\alpha_{T_c}(T_c) = \alpha_\Delta [2T_{c,0}/T_c - 1]$, where $T_{c,0} = \beta\Delta_0/k_B$ and $\beta = a_0\chi_s$, here χ_s is the static spin susceptibility. These results then point to an isotope effect $\alpha_\Delta \approx 0.06$ which remains approximately independent of doping across the superconducting phase curve. (The data in Figure 3-9 may suggest that α_Δ decreases a little with underdoping but there is little consistency among the various data sources at low T_c that could strongly justify this conclusion.) A similar value is obtained for $\text{La}_{2-x}\text{Sr}_x\text{CuO}_4$ (La214) and Y124. In the BCS model with phonon-mediated pairing, it would be expected that $\alpha_{T_c} = \alpha_\Delta = 0.5$, which is clearly not the case. But this depends on the relevant mass used in defining α_{T_c} and the magnitude of Coulomb repulsion. If the acoustic modes were important, then the total mass might be approximated by the unit cell mass. Then, α_Δ is indeed found to be about 0.5 and constant more or less independent of the hole concentration. More likely, the relevant electron-phonon coupling is associated with the optical branches, consistent with the high T_c 's. Theoretical calculations indicate that that plane-oxygen phonon modes enhance d-wave superconductivity [77].

T.Dahm [83] studied the influence of a phenomenological pseudogap on the isotope exponent in the weak-coupling limit, the linearized gap equation for an anisotropic pairing interaction $V(\bar{k}, \bar{k}')$ reads

$$\Delta(\bar{k}) = \sum_{\bar{k}'} V(\bar{k}, \bar{k}') \frac{\tanh(\varepsilon_{\bar{k}'} / 2T_c)}{2\varepsilon_{\bar{k}'}} \Delta(\bar{k}') \quad (3.48)$$

Here, $\varepsilon_{\bar{k}}$ is the band dispersion and $\Delta(\bar{k})$ the superconducting gap function.

The pairing interaction consists of two parts: a phononic part $V_p(\bar{k}, \bar{k}')$ and an electronic part $V_e(\bar{k}, \bar{k}')$, such that $V(\bar{k}, \bar{k}') = V_p(\bar{k}, \bar{k}') + V_e(\bar{k}, \bar{k}')$. The dominant contribution shall be V_e . Then, in weak-coupling approximation he used

$$V_e(\bar{k}, \bar{k}') = \begin{cases} V_{e0} \psi_\eta(\bar{k}) \psi_\eta(\bar{k}') & \text{if } |\varepsilon_{\bar{k}}|, |\varepsilon_{\bar{k}'}| \leq \omega_e \\ \mathbf{0} & \text{else,} \end{cases} \quad (3.49)$$

where Ω_e is the characteristic energy scale of the electronic part and is assumed to be independent of isotopic mass. $\psi_\eta(\bar{k})$ is the basis function for the pairing symmetry considered. For s-wave pairing $\psi_s(\bar{k}) = 1$, for $d_{x^2-y^2}$ - wave pairing $\psi_{d_{x^2-y^2}}(\bar{k}) = \cos 2\Theta_{\bar{k}}$, and for d_{xy} - wave pairing $\psi_{d_{xy}} = \sin 2\Theta_{\bar{k}}$, where $\Theta_{\bar{k}} = \arctan(k_y/k_x)$ is the angular direction of the momentum \bar{k} .

The phononic part may consist of different contributions having different symmetries. However, since he assumed that the electronic part is dominating with a symmetry specified by $\psi_\eta(\bar{k})$, only the $\psi_\eta(\bar{k})$ component of V_p , having the same symmetry, will affect T_c . Therefore he assumed without loss of generality

$$V_p(\bar{k}, \bar{k}') = \begin{cases} V_{p0} \psi_\eta(\bar{k}) \psi_\eta(\bar{k}') & \text{if } |\varepsilon_{\bar{k}}|, |\varepsilon_{\bar{k}'}| \leq \omega_p \\ \mathbf{0} & \text{else,} \end{cases} \quad (3.50)$$

where ω_p is the characteristic phonon energy. In the harmonic approximation, ω_p varies with the isotopic mass M like $1/(M)^{1/2}$, while Ω_e is assumed to be independent of M .

For such an interaction the gap function can be separated into two parts:

$$\Delta(\bar{k}) = \Delta_p(\bar{k}) + \Delta_e(\bar{k}), \quad \text{with}$$

$$\Delta_{e,p}(\bar{k}) = \begin{cases} \Delta_{e0,p0} \psi_\eta(\bar{k}) & \text{if } |\varepsilon_{\bar{k}}| \leq \omega_{e,p} \\ \mathbf{0} & \text{else.} \end{cases} \quad (3.51)$$

With this condition, Eq.(3.48) becomes a 2x2 matrix equation for the two order-parameter components Δ_{e0} and Δ_{p0} . Assuming a cylindrical Fermi surface with a constant density of states, Eq.(3.48) can be written in the form

$$\begin{bmatrix} \Delta_{eo} \\ \Delta_{po} \end{bmatrix} = \begin{bmatrix} V_{eo}L(\omega_e) & V_{eo}L(\omega_e) \\ V_{po}L(\omega_e) & V_{po}L(\omega_p) \end{bmatrix} \begin{bmatrix} \Delta_{eo} \\ \Delta_{po} \end{bmatrix} \quad (3.52)$$

where he defined the function $L(\Omega)$

$$L(\omega) = N(\mathbf{0}) \int_0^{\omega} d\varepsilon \frac{\tanh(\varepsilon/2T_c)}{\varepsilon} \approx N(\mathbf{0}) \ln\left(\frac{1.13\omega}{T_c}\right) \quad (3.53)$$

The last expression holds in the weak-coupling limit $\Omega \gg T$. $N(0)$ denotes the density of states at the Fermi level. In deriving Eq. (3.52) he assumed $\omega_e \leq \omega_p$. Letting $L_p = L(\omega_p)$ and $L_e = L(\omega_e)$ the leading eigenvalue of the matrix in Eq.(3.52) is

$$\lambda(\omega_e, \omega_p, T) = \frac{V_{eo}L_e + V_{po}L_p}{2} + \frac{1}{2} \sqrt{(V_{eo}L_e - V_{po}L_p)^2 + 4V_{eo}V_{po}(L_e)^2} \quad (3.54)$$

and T_c is determined from the implicit equation

$$\lambda(\omega_e, \omega_p, T_c) = 1 \quad (3.55)$$

From this the isotope exponent α can be calculated :

$$\alpha = \frac{1}{2} \frac{d \ln T_c}{d \ln \omega_p} = -\frac{1}{2} \frac{\omega_p}{T_c} \frac{\frac{\partial \lambda}{\partial L_p} \frac{\partial L_p}{\partial \omega_p}}{\frac{\partial \lambda}{\partial L_p} \frac{\partial L_p}{\partial T_c} + \frac{\partial \lambda}{\partial L_e} \frac{\partial L_e}{\partial T_c}} \quad (3.56)$$

In the weak coupling limit $\omega_p, \omega_e \gg T_c$, this gives

$$\alpha = \frac{1}{2} \frac{V_{po}(1 - V_{eo}L_e)}{V_{po}(1 + V_{eo}L_e) + V_{eo}(1 - V_{po}L_p)} \quad (3.57)$$

For a purely electronic interaction $V_{po} = 0$ this expression yields $\alpha = 0$ and for a purely phononic interaction $V_{eo} = 0$ it gives $\alpha = 0.5$, as one should expect. For a mixed interaction α_0 will generally be between 0 and 0.5. In fact, one can easily show that for

given values of Ω_p and Ω_e one can always choose V_{p0} and V_{e0} in such a way that a given value of T_c and $\alpha \in [0,0.5]$ is reached.

Now we wish to consider the influence of a pseudogap. In the presence of a pseudogap we have to modify the single-particle excitation spectrum. Following Williams and co-workers [84], we replace

$$\varepsilon_{\bar{k}} \text{ in Eq.(3.48) by } \sqrt{(\varepsilon_{\bar{k}})^2 + (E_g(\varepsilon_{\bar{k}}))^2} \quad (3.58)$$

where $E_g(\bar{k})$ is the pseudogap and will be chosen to be either $E_{g,s}(\bar{k}) = E_{g0} =$ constant for an s-wave pseudogap or $E_{g,d}(\bar{k}) = E_{g0} \cos 2\Theta_{\bar{k}}$ for a d-wave type pseudogap. Note that this symmetry of the pseudogap does not necessarily have to be identical with the pairing symmetry. However, the study in 84 suggests that both symmetries are of d-wave type in underdoped high- T_c compounds. With the replacement Eq.(3.58) the function L becomes

$$L(\omega) = \frac{N(0)}{2\pi} \int_0^{2\pi} d\Theta \psi_{\eta}^2(\Theta) \int_0^{\omega} d\varepsilon \frac{\tanh(\sqrt{\varepsilon^2 + (E_g(\Theta))^2} / 2T_c)}{\sqrt{\varepsilon^2 + (E_g(\Theta))^2}} \quad (3.59)$$

Equations (3.54) and (3.56) still remain valid, if one uses this expression for L(ω). In the weak-coupling limit, $\Omega_p, \Omega_e \gg T_c, E_g$ we then find for the isotope exponent

$$\alpha = \alpha_0 \left(\frac{1}{4\pi T_c} \int_0^{2\pi} d\Theta \int_0^{\infty} d\varepsilon \frac{\psi_{\eta}^2(\Theta)}{\cosh^2(\sqrt{\varepsilon^2 + (E_g(\Theta))^2} / 2T_c)} \right)^{-1} \quad (3.60)$$

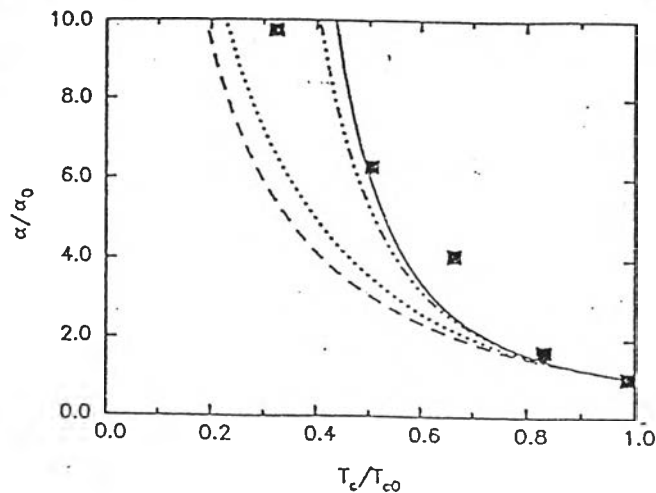


Figure 3-9: Weak coupling result for the isotope exponent α/α_0 as a function of T_c/T_{c0} in the presence of a pseudogap. [83]

here α_0 is the isotope exponent Eq.(3.57) in the absence of a pseudogap. Equation (3.60) shows that α/α_0 only depends on E_{g0}/T_c , the pairing symmetry $\psi_\eta(\Theta)$ and the symmetry of the pseudogap. Since T_c is a function of E_{g0} , determined from Eq.(3.55), for a given symmetry of both the pseudogap and the pairing state α/α_0 is a universal function of T_c/T_{c0} . Here, $T_{c0} = T_c(E_g=0)$. Figure 3-9 [84] shows α/α_0 as a function of T_c/T_{c0} for different symmetries. The solid line shows the isotope exponent for an s-wave pseudogap. This result is independent of the pairing symmetry, as can be seen by performing the angular integration in Eq.(3.60). For an anisotropic pseudogap having $d_{x^2-y^2}$ - wave symmetry, however, the pairing symmetry does affect the result. The dotted line shows the result for an s-wave superconductor with a $d_{x^2-y^2}$ - wave pseudogap, while the dashed-dotted line shows the results for a $d_{x^2-y^2}$ - wave superconductors with a $d_{x^2-y^2}$ - wave pseudogap. The weakest T_c/T_{c0} dependence is found for a d_{xy} superconductor with a $d_{x^2-y^2}$ - wave pseudogap (dashed line). In all cases one can see from Eq.(3.32) that α/α_0 diverge for $T_c \rightarrow 0$. Thus in principle arbitrarily high values of α can be reached. As an illustration, experimental results on Pr-doped YBCO are shown in figure 3-9 as solid squares [71]. Certainly these differences need further explanation and cannot be understood solely due to the influence of a pseudogap, moreover the isotope exponent in Eq.(3.32) that was found in 83 is not an exact expression, we therefore wish to reconsider the isotope effect in the presence of a pseudogap and attempt to predict the phenomenon quantitatively with the exact solutions. The theoretical formulation will be given and the numerical results will be shown in the next chapter.